# Two-step principal component analysis (PCA) as a method for separating auditory N1 and N250 elicited from 9-year-old children using a dense electrode array:

# Comparison between ERP-PCA and CSD-PCA

Riikka Pantsar
Master's thesis
University of Jyväskylä
Department of Psychology
February 2008

| | |
|---|---|
| **Supervisor of the graduate thesis** | Paavo H.T. Leppänen, Docent, Ph.D., Academy Research Fellow<br>Department of Psychology,<br>University of Jyväskylä, Finland |
| **Co-supervisor** | Jarmo Hämäläinen, M.A.,<br>doctoral student<br>Department of Psychology,<br>University of Jyväskylä |
| **Research projects** | *Jyväskylä Longitudinal Study of Dyslexia* (JLD, funded by Academy of Finland) |
| **Research site** | Centre of Excellence for Human Development and Risk Factors,<br>Department of Psychology,<br>University of Jyväskylä, Finland |
| **Supported by** | Academy of Finland,<br>Eemil Aaltonen Foundation,<br>Department of Psychology<br>University of Jyväskylä, Finland |

JYVÄSKYLÄN YLIOPISTO
Psykologian laitos
Riikka Anneli Pantsar

**Tiheällä elektrodiverkolla 9-vuotiailta lapsilta mitattujen auditoristen N1 ja N250 komponenttien erottelu kaksivaiheisella pääkomponenttianalyysilla (PCA): Vertailussa ERP-PCA ja CSD-PCA**

Pro Gradu –tutkielma, 31 sivua
Ohjaaja: Paavo H. T. Leppänen, dosentti, PsT, akatemiatutkija
Psykologia
Helmikuu 2008

Tässä tutkimuksessa selvitettiin kaksivaiheisen pääkomponenttianalyysin (PCA) kykyä erotella lähekkäisiä tai päällekkäisiä auditorisia herätevastekomponentteja (ERP). Kahta eri PCA sovellusta – ERP-PCA:ta ja CSD-PCA:ta – tutkittiin, ja niiden tuloksia vertailtiin. Aineisto kerättiin kahdeltakymmeneltä 9-vuotiaalta lapselta tiheällä elektrodiverkolla. Näin saadut ERP käyrät muutettiin lisäksi CSD käyriksi (toinen spatiaalinen derivaatta; Laplacian), ja aineistot analysoitiin rinnakkain. Aineistoista tutkittiin eksogeenisiä N1 ja N250 komponentteja ja niiden herkkyyttä ärsykkeiden esitystiheydelle (ISI). *Lyhyen ISI*:n tilanteessa *'atta'* ärsykkeitä esitettiin 610 ms ISI:lla, kun taas *pitkän ISI*:n tilanteessa ärsykkeet esitettiin näennäis-satunnaisesti 1-5 sekunnin välein. Molemmat PCA sovellukset kykenivät erottelemaan N1:n, N250:n ja niiden alakomponentteja. Sekä ERP- että CSD-PCA erottelivat aineistoista kaksi N1 alakomponenttia, epäspesifin N1:n ja T-kompleksin, jotka olivat aktiivisia molemmilla esitystiheyksillä. Kumpikaan menetelmä ei erotellut aineistoista kolmatta N1 alakomponenttia, N1b:tä. CSD-PCA aineistossa oli viitteitä N250:n herkkyydestä esitystiheyden muutoksille, mutta näitä viitteitä ei löytynyt ERP-PCA aineistosta. Lisäksi CSD-PCA aineistosta löytyi N250:lle positiivinen, radiaalinen alakomponentti, joka muistutti T-kompleksin Ta komponenttia. Vaikka ERP-PCA:n ja CSD-PCA:n erottelemien komponenttien rakenteissa oli samankaltaisuuksia, CSD-PCA:n erottelemat komponentit antoivat tarkemman ja yksityiskohtaisemman kuvan aineiston temporaalisesta ja spatiaalisesta jakaantumisesta. Kaksivaiheinen PCA vähensi huomattavasti 129 elektrodin tuottaman tiedon määrää, helpottaen näin ollen olennaisten komponenttien valintaa jatkoanalyyseihin.

# Two-step principal component analysis (PCA) as a method for separating auditory N1 and N250 elicited from 9-year-old children using a dense electrode array: Comparison between ERP-PCA and CSD-PCA

Riikka A. Pantsar

*Department of Psychology, University of Jyväskylä, PL 35 (Agora Center), 40014 Jyväskylän Yliopisto*

February 2008

---

**Abstract**

The separation of close or overlapping auditory event-related potential (ERP) components was investigated by the means of two-step principal component analysis (PCA). Two solutions within PCA – ERP-PCA and CSD-PCA – were applied and compared. The data was recorded from twenty 9-year-old children with a dense array of 129 electrodes. The obtained ERP waveforms were additionally transformed into spherical spline current source density (CSD) waveforms, and the data were analyzed in parallel. Exogenous N1 and N250 components and their sensitivity to changes in inter-stimulus-interval (ISI) were examined. In the *short ISI condition* the naturally produced *'atta'* stimuli were presented with a constant ISI of 610 ms, whereas in the *long ISI condition* they were played at pseudo-random intervals of 1-5 s. PCA components corresponding to N1, N250 and their subcomponents were extracted by both solutions. Both ERP- and CSD-PCA disentangled two N1 subcomponents, non-specific N1 and T-complex, which were active with both ISIs. No frontocentral N1b was extracted by either of the solutions. There was evidence of ISI sensitivity for N250 in the CSD-, but not in the ERP-PCA data. Additionally, a positive radial subcomponent, equivalent to the Ta of T-complex, was distinguished for N250 in the CSD-PCA data. Although similarities between the component structures between ERP- and CSD-PCA solutions were evident, CSD-PCA produced sharper and more detailed summary about the temporal and topographical distribution of the ERP data. Using a two-step PCA considerably reduced the amount of information obtained by the 129 electrodes, facilitating the selection of relevant components for further analyses.

*Keywords*: Event-related potential (ERP); Principal component analysis (PCA); Current source density (CSD); Children; N1; N250; Inter-stimulus-interval (ISI)

---

## 1. Introduction

The application of different methodological approaches to event-related potentials (ERPs) can have substantial effects on the conclusions made from the data. As the ERP measurement techniques have developed from low-density and midline recordings to extensive multiple channel recordings, the traditional analyzing methods, such as peak measurement, are no longer able to handle the complexity of the growing amount of data. In addition, the development of data collection equipment enables more accurate and less noise-affected recording of event-related potentials. New, reliable analyzing methods for ERP data are needed to get more detailed and profound information about the nature of ERP components.

In this study, the methodological possibilities of principal component analysis (PCA) applied into a high-density (128-channel) ERP data are considered. PCA is a comprehensively studied, 'data-driven' technique, and its applicability to electroencephalographic (EEG) data has been acknowledged widely among researchers. PCA utilizes all the information from 128 channels, and is thereby able to identify components not necessarily even visible in the grand averages of ERP data (Kayser & Tenke, 2006a). However, opinions still differ as to how and what kind of different PCA algorithms and solutions should be used. The introduction of a new CSD-PCA method (Tenke & Kayser, 2005) called forth the need for its comparison with more traditional PCA methods. Accordingly, a comparison of two different PCA methodologies' ability to extract physiologically relevant components from (maturational) ERP data is of interest in this present study. Next, a brief review of the studied ERP components and their maturation is introduced, followed by a presentation of principal component analysis of ERP data.

***Maturation of the ERP components N1 and N250***. Event-related potentials (ERPs) are distinctive time-locked deflections on an averaged EEG trace produced by repeated presentation of stimuli. ERP components are considered to be contributions of localized physiological generators to the ERP waveform, activated by the stimuli (Näätänen & Picton, 1987). The definition of different components is somewhat ambiguous and difficult due to the fact that the ERP waveform is a sum of spatially and temporally overlapping post-synaptic brain potentials. Thus, components are not merely positive or negative waves visible in an averaged trace, but rather a set of arithmetical summations of activity underlying those peaks and throughs (Näätänen, 1992). Multiple generators contribute to the scalp-recorded components and they are, accordingly, composed of several overlapping subcomponents.

ERP components are traditionally classified into exogenous and endogenous components on the account of their characteristics. Exogenous components are obligatory and determined by an external stimulus, whereas endogenous components depend on the subject's intentions and are usually elicited in the absence of external stimuli (Donchin, Ritter, & McCallum, 1978). Subsequently, a more detailed classification has been suggested by Näätänen (1989). It separates components into six categories called sensory-specific obligatory, activational, integrative, executive, motorspecific and anticipatory components. ERP components are labeled by polarity (P = positive, N = negative), followed by an ordinal number or the number indicating the latency of a component in milliseconds.

This study concentrated on two obligatory negative ERP components in children (N1 and N2; also referred to as N250), both of which have an early onset latency and are evoked by the presentation of distinct stimuli without active attention. Motivation for the investigation of these particular components was that early ERP components have the largest amplitudes and are consequently relatively easy to detect. Moreover, the spatial and temporal proximity of the components in question is a challenge for PCA and thereby an interesting research area. In addition, the employed research paradigm, which did not demand active attention or performance, seemed reasonable in the case of children subjects.

There are marked differences between ERP component structures of children and adults (Johnstone, Barry, Anderson, & Coyle, 1996; DeFrance, Sands, Schweitzer, Gingsberg, & Sharma, 1997; Ponton, Eggermont, Kwong, & Don, 2000; Albrecht, von Suchodoletz, & Uwer, 2000; Ceponiené, Rinne, & Näätänen, 2002; Ceponiené, Alku, Westerfield, Torki, & Townsend, 2005). Maturation has an affect on the amplitude and latency of components. However, there is no clear consensus on whether, or how, components from different maturational stages correspond with each other. Also the rate in which stimuli are presented, as well as the chosen research paradigm, has an effect on the elicited ERP components. Defining all the known ERP components and their maturation processes is beyond the scope of this study, and thus, only the negative components crucial to the employed oddball paradigm are defined next in detail.

The basic idea of an auditory oddball paradigm is to present at least two different kinds of stimuli to the subject. The more frequent ones are called standards and the infrequent ones deviants. In adults, a N1-P2 vertex complex is usually elicited as a response to standard tones, preceded by a small P1 component (Näätänen, 1992). The N1 component is, accordingly, considered as a level change detection component (Picton, Alain, Otten, Ritter, & Achim, 2000), which is elicited whenever the central nervous system detects a stimulus. The adult N1 is dominated by a non-specific subcomponent, originated from the frontal motor and premotor cortices. It includes also a radially oriented subcomponent called T-complex (N1c), generated in the lateral surface of the auditory cortex and a frontocentral N1b subcomponent, generated by a vertically oriented dipole in the supratemporal plane of the auditory cortex (Gomes et al, 2001). Topographically, the non-specific N1 is maximal posterior to the scalp distribution of the frontocentral N1b (Ponton et al., 2000). T-complex is composed of three subcomponents (i.e. N1a, Ta and Tb), from which the focus in this study is on the negative Tb, only visible at the temporal leads ~ 45 ms after N1 (Gomes et al., 2001; Tonnquist-Uhlen, Ponton, Eggermont, Kwong, & Don, 2003). To deviant tones, a frontally or frontocentrally maximal N2 component is additionally elicited, from which a specific integrative mismatch negativity (MMN) component can be isolated (Näätänen, 1992). Interestingly, Kayser, Tenke and Bruder (1998) found N2 to be maximal at central and *temporal* sites in adults.

In children, the corresponding components to rapidly presented sounds are P150, N250, N450 – the numbers indicating the longer latency range of components compared to those of adults – and do not become adult-like until the age of 16-18 years (Ceponiené et al., 2001; 2005). According to previous research, it seems that children's N250 component overlaps the adult-like N1 and P2 components (Johnstone et al., 1996; Ceponiené et al., 2002). In fact, unlike in children, no N2 is elicited in adults either to standard or unattended stimuli (Johnstone et al., 1996; Karhu et al., 1997). Interestingly, Johnstone et al. (1996) found that the amplitude, latency and frontal scalp distribution of N250 in children did not differ between standard and target stimuli. It was also concluded that while the N250 latency to target stimuli did not change significantly with age, the amplitude did decrease. Similar findings were reported by Ceponiené, Cheour and Näätänen (1998) and Ceponiené et al. (2002). Yet, Ponton et al. (2000) found that N250 component increased in latency as a function of age at central electrodes, but showed no age-related change at frontal electrodes. Consequently, when other ERP component latencies shorten with age, N250 wave diminishes and N1 wave becomes visible, along with P2 (Johnstone et al., 1996). Some researchers assume that adult N1 is equivalent to the child N250 component (Kurtzberg, Vaughan, Kreuzer, & Fliegler, 1995; Ceponiené et al., 2001), whereas others have concluded that children's N250 resembles that of adult N2 (Johnstone et al., 1996; Ceponiené et al., 1998; 2002). However, the maturational process of ERP components continues to some extent up to adolescence, and before that the N1 component is not consistently present (Ponton et al., 2000).

However, when interstimulus-intervall (ISI) duration exceeds 1s, N1 can also be seen in younger children. It was suggested by Gomes et al. (2001) that in this case, the observed component actually consists of N1 subcomponents T-complex and N1b, whereas the T-complex is observable from early childhood even with short ISIs. Karhu et al. (1997) found topographically separate parallel processing in children in form of different ERP components recorded at Cz and T3 electrodes with an ISI of 1s. At Cz, a decreasing N1 wave was observed accompanied with an increasing N2 wave. At temporal electrode (T3) only N1 response was found, although slightly longer in latency and larger in amplitude than at Cz. These two N1 components could be justifiably referred to as N1b (Cz) and T-complex (T3). Additionally, in a study examining the effects of ISI prolongation to the exogenous ERP components, it was found that when ISI duration was 700 ms or longer, a distinct frontocentral N160 component was separable from the N250 component in 5-7-year-old children (Ceponiéne et al., 1998). The authors assumed this to be – not similar but – equivalent to the adult N1 component. They also observed a temporally negative component N190, peaking 26-30 ms later than the N160, and concluded that these two components correspond the subcomponents of adult N1 (i.e. N1b and T-complex). In a subsequent study, however, Ceponiené et al. (2002) argue that it is the non-specific subcomponent of N1 that is observable in young children when stimuli are presented at a slow rate, and with rapid stimulus presentation N1 is revealed only when the slow activity is filtered out from the data. Furthermore they, as many others (e.g. Albrecht et al., 2000; Ponton, Eggermont, Khosla, Kwong, & Don, 2002), suggested that children's N1 has a protracted maturational course and is composed of differentially weighed subcomponents than adult N1.

The aforementioned, simultaneously occurring processes in topographically different parts of the brain, issues a challenge to the analysis of auditory ERPs. Ponton et al. (2000) suggested that analyzing responses from a single electrode is not adequate, because observed auditory responses are crucially dependent on the scalp location at which they are recorded. More accurate ERP data can be acquired through dense electrode arrays, but the amount of information, then, is too overwhelming to peak measurement analysis. Consequently, these findings support the use of high-density electrode array providing information extensively from different scalp locations. They also encourage researchers towards the use of analyzing methods, which enable the revelation of both temporal and spatial aspects of different components and subcomponents. When it comes to child ERP data, the objectivity provided by the more sophisticated 'data-driven' methods is especially crucial, because particularly around age 10 abrupt step-like decreases take place in the amplitude of component complexes and the temporal and spatial structure of ERP components change as a function of development and maturation (Ponton et al., 2000; Bishop, Hardiman, Uwer, & von Suchodoletz, 2007). Accordingly, a two-step principal component analysis (e.g. van Boxtel, 1998; Spencer, Dien, & Donchin 2001; Dien, Spencer, & Donchin, 2003) is the approach utilized here as an attempt to extract spatially and temporally overlapping negative components of auditory ERP data.

***Principal component analysis of ERP data.*** The concept of principal component analysis (PCA) belongs to a class of factor-analytic procedures (van Boxtel, 1998; Dien & Frishkoff, 2005). PCA is based on a second-order covariance or correlation matrix, which it decomposes into orthogonal linear combinations (i.e. components). Thus, PCA summarizes the complex relations of the original data, in a decreasing order, into a small number of components, most efficiently explaining the variation between all variables. From the initial association matrix, a certain number of components are retained and rotated, on the ground of chosen extraction criterion, to obtain a simpler interpretation of the components (e.g. Chapman & McCarthy, 1995; van Boxtel, 1998; Dien, Beal, & Berg, 2005). The two most commonly used methods are orthogonal rotation (e.g. Varimax), producing independent factors and oblique rotation (e.g. Promax), producing correlated factors. After rotation, PCA assigns factor loadings and scores.

As a tool for the study of ERPs, PCA was advocated by Donchin in 1966. It can be used as a pre-processing method for raw EEG data for the purposes of e.g. ocular artefact rejection (e.g. Wallström, Kass, Miller, Cohn, & Fox, 2004; Casarotto, Bianchi, Cerutti, & Chiarenza, 2004). It is also widely used as an explorative analysis for averaged or raw EEG data (e.g.; Kayser et al., 1998, 2006, Spencer, Dien, & Donchin, 1999, 2001; Richards, 2004). In ERP data, the variables are microvolt readings either at consecutive time points (temporal PCA) or at each electrode (spatial PCA). The major source of covariance is assumed to be the ERP components (Dien & Coles, 1991). According to Delorme and Makeig (2004), rotation methods are in fact applied after the basic PCA analysis, because the electrical activity in the brain is nearly always non-orthogonal and overlapping, contrary to the assumptions of PCA. Generally speaking, the purpose of rotation is to reduce temporal and spatial overlap of the components (van Boxtel, 1998). Only some researchers support the use of Promax (Dien et al., 2003, 2005), while the conventional Varimax criterion is preferred by others (Kayser & Tenke, 2003; Beauducel & Debener, 2003; van Boxtel, 1998). Dien et al. (2003, 2005) argue that when using temporal PCA for ERP datasets, the latent variables are significantly correlated due to the scalp topography (3-dimensional), and thus recommend the use of Promax rotation. On the other hand, Kayser and Tenke (2005) note that even though oblique rotations (e.g. Promax) may achieve a grater degree of simple structure, Varimax-rotated components are more concise and accurate.

There are, accordingly, many decisions to be made before the application of PCA, concerning the selection of association matrix, algorithm, rotation method and extraction criteria. Various combinations of algorithms and solutions are possible, but only a few of them have become well established in the field of ERP research. Traditionally, a temporal PCA is applied followed by a Varimax rotation (Beauducel & Debener, 2003; Delplanque, Silvert, Hot, & Sequeira, 2005; Kayser & Tenke, 2003, 2006a, 2006b; Kayser et al., 1998, 2006). When using a dense electrode array, a two-step approach (e.g. spatiotemporal PCA) has been recommended by researchers, for it allows a greater reduction in the dimensionality of the data set and helps to disentangle spatially and temporally overlapping ERP components (e.g. Spencer et al., 2001; Dien et al. 2003).

Recently, Tenke & Kayser, (2005) have introduced a new CSD-PCA technique, which operates on spherical spline current source density (CSD; second spatial derivative; Laplacian) maps instead of ERP scalp topographies (e.g. Law, Rohrbaugh, Adams, & Eckardt, 1993). CSD is a mathematical transformation, which represents the magnitude of the radial current flow entering (sinks) and leaving (sources) the scalp (Nunez, 1981). CSD waveforms are reference-free transformations of the original ERP waveforms (Kayser & Tenke, 2006a, 2006b). In the CSD-PCA technique, ERP waveforms are transformed into CSD waveforms and analyzed with PCA. The concept of CSD maps in ERP studies is not novel per se (e.g. Tenke et al., 1998; Gomot, Giard, Roux, Barthélémy, & Bruneau, 2000; Gomes et al., 2001). However, the combination of CSD and PCA methodologies has not been examined until the last few years. Results have been promising concerning the use of temporal PCA for CSD waveforms to identify ERP generator patterns (Kayser & Tenke, 2006a; 2006b; Kayser et al., 2006). As argued by the researchers, the superiority of the combined CSD-PCA solution is based on the production of sharper and simpler topographies without the ambiguities of recording reference.

Like traditional ERP measurement techniques, also PCA has its shortcomings. The risk of misallocation of variance (e.g. Wood & McCarthy, 1984; Beauducel & Debener, 2003), low signal-to-noise ratios, outliers and latency jitter (e.g. van Boxtel, 1998; Chapman & McCrary, 1995) can reduce the reliability of PCA-derived component measures. However, these limitations are well-known and made explicit, which leads to a cautious and critical consideration of the obtained results. Additionally, the correspondence between principal components and ERP components has been criticized, and this relationship should always be interpreted and stated with caution. Moreover, the placement of the recording reference essentially impacts the polarities, amplitudes and peak latencies of recorded ERP components. To solve this problem, the above mentioned current source density (CSD) transformation algorithm providing a reference-free representation of current generators that underlie ERP topography has been proposed (Nunez, 1981).

The use of a 129-electrode Geodesic Sensor Net (EGI, Inc., Eugene, OR) (Tucker, 1993) requires the application of more efficient methods to enable the most optimal utilization of the information. Here, ERP waveforms and their CSD transformations were analyzed with a two-step principal component analysis (PCA).

***Objective***. The goal of this study was to explore, if a two-step principal component analysis (PCA) could extract temporally and spatially close or overlapping auditory brain responses (ERPs) measured with 129-electrode Geodesic Sensor Net (EGI, Inc., Eugene, OR) (Tucker, 1993). Two different solutions within temporospatial PCA – ERP-PCA and CSD-PCA – were applied and their outcomes compared. Focus was on the exogenous (i.e. obligatory) unattended negative auditory ERP components N1 and N250 elicited from healthy 9-year-old children. In addition, the correspondence of the extracted PCA components to the actual ERP components was discussed.

As suggested by many researchers (e.g. Dien et al., 2003; Spencer et al., 2001; van Boxtel, 1998) a two-step PCA is crucial when analyzing data from dense electrode arrays. Yet, ERP studies using high density electrode arrays and the recommended two-step PCA approach are continually quite scarce. Methodological research of the recently proposed new CSD-PCA technique has been restricted to temporal PCA (Tenke & Kayser, 2005; Kayser & Tenke, 2006a, 2006b). The objective here was to explore, if there are significant differences between the component structures extracted by the traditional ERP-PCA and the novel CSD-PCA. It was hypothesized that the CSD-PCA, operating with sharper and more distinct scalp topographies would surpass the more traditional ERP-PCA solution in accuracy.

The properties of the two methodological solutions were compared by applying them to the ERP data elicited from healthy children with different inter-stimulus-intervals (ISIs). Considering the age of the children (9 years), it was assumed that the applied research paradigms would elicit different subcomponents of the N1 and the N250 component in the *long ISI condition*. In the *short ISI condition*, N1 was not expected to be elicited, but N250 – similar to the one observed in the *long ISI condition* – was thought to be visible. Thus, the ability of ERP- and CSD-PCA to separate ERP components specific to the *long* and *short ISI conditions*, and the separation of N1 subcomponents and N250 from each other, was investigated and compared. This was assumed to be a challenge for PCA due to temporal and spatial overlap of the components. There is, however, support for the PCA technique in such cases (Richards, 2004).

Along with the development of ERP measurement techniques, also requirements for more sophisticated analyzing methods arise. The main purpose of this study was to obtain cumulative support for the use of ERP-PCA and CSD-PCA methodologies in event-related potential research by investigating their use in an unparalleled fashion.

## 2. Methods

### *2.1. Participants*

Appropriate subjects considering this particular study were selected among the participants of The Jyväskylä Longitudinal Study of Dyslexia. The JLD-project commenced in 1993, investigating approximately 200 families in the area of Jyväskylä, half of which had a family history of dyslexia and the other half did not (Leinonen et al., 2001).

Altogether twenty EEG data sets (9 boys, 11 girls; 3$^{rd}$ grade; mean age 9,4; range: 9,1-9,8) from the original research were accepted to this study. They were all collected from control subjects with normal reading skills and no familial risk for dyslexia.

*2.2. Stimuli and procedure*

The experimental design of the JLD-project was an auditory oddball (3 conditions) and EQ paradigm (control condition) for 3rd graders. Two of the oddball conditions consisted of naturally produced speech stimuli (see Fig. 1). In addition, there was one condition with non-speech stimuli. Lastly, a control condition (EQ paradigm) with speech and non-speech stimuli to make sure that the differences in the oddball paradigm were not due to a compulsory response to the stimuli, but a real detection of change. For the purposes of this particular study, expedient stimuli were selected from the two speech experiments and from the control experiment.

There were four different kinds of stimuli in the speech conditions *('ata', 'atta', 'apa', 'appa')*. In the first experiment *'ata'* was used as a standard (probability 0.8) and *'atta'* and *'apa'* were deviant stimuli (probability 0.1). In the second, otherwise similar, experiment *'atta'* was standard and *'ata'* and *'appa'* were deviant stimuli. In both conditions there were altogether 1250 stimuli presented with a constant ISI (off-set to on-set) of 610 ms in five consecutive blocks. For the analyses of this study, two standard *'atta'* stimuli (*'atta'* following *'ata'* i.e. */s8dt-satta/*, and *'atta'* following *'apa'* i.e. */s8dp-satta/*) along with the deviant *'atta'* (i.e. */dat8-datta/*) and deviant *'appa'* (i.e. */dap8-dappa/*) were selected. These stimuli are henceforth referred to as stimuli of the *short ISI condition*.

In the control condition (EQ paradigm), all of the stimuli (including non-speech stimuli) were placed to the same experiment and played at pseudo-random intervals of 1-5 seconds with equal probability. However, only the two speech stimuli (*'atta'* i.e. */ata8-datta8/* and *'appa'* i.e. */apa8-dappa8/*) from the control condition were included to the analyses of this study. The chosen control stimuli are henceforth referred to as stimuli of the *long ISI condition*.

During the experiment children were sitting in a chair watching soundless cartoons of their own choice or playing a simple videogame. They were asked to ignore the noises. To secure the well-being of children, they were visually monitored and short snack or stretching pauses were taken whenever necessary. The duration of the experiment was approximately three hours.

*2.3. EEG recording and averaging*

Scalp EEG was recorded and stored with Net Station 2.0 using a High-density Geodesic Sensor Net (EGI) with 129 electrodes (www.egi.com/c_120_eegtech.html). Continuous EEG data was online filtered using a 0.1 Hz highpass and 100 Hz lowpass filters, with a sampling rate of 500 Hz. Data was referenced to the vertex electrode and then re-referenced using an average reference. Impedances for most of the electrodes were kept below 50 kΩ. For the few electrode locations where the impedance was higher, EEG quality was visually ensured. EEG-channels with excessive electric or other extra-cerebral noise were marked and later interpolated (see below). The vertex was used as a reference electrode during recording. Stimulus trigger codes were recorded online with the EEG.

The recorded EEG data was analyzed with Besa 5.1.6. (www.besa.de/index_home.htm). Before averaging, artifacts were scanned with the offline filters set to 0.53 Hz for the low cutoff (6 dB/forward) and the notch filter to 50 Hz, width 2 Hz. Trials with peak-to-peak deflections exceeding 200 μV (extra-cerebral artifacts, including noise from electric devices, movement or tension-related noise etc.) were excluded from the analyses, along with the channels that were bad during the whole experiment. Blink correction was done by using an individual eye blink correction method by BESA (Hämäläinen, J. A., Leppänen, P. H. T., Guttorm, T. K., & Lyytinen, H., 2007). Altogether 20-200 blinks were averaged. Next, trials were averaged separately for each stimulus type. Before further analysis, all the previously marked bad channels were spherical spline interpolated (Perrin et al., 1989, 1990) and averages were digitally filtered (high cutoff 35 Hz/12 dB zero) (see BESA tutorial: www.besa.de/index_home.htm?/tutorials/index_viewlets_intro.htm).

Before PCA analyses, all averaged ERP waveforms from 20 participants were also transformed into current source density (CSD) estimates using the spherical spline surface Laplacian algorithm (Perrin et al. 1989, 1990). As a result, two different data sets - the other with ERP and the other with CSD waveforms - were obtained.

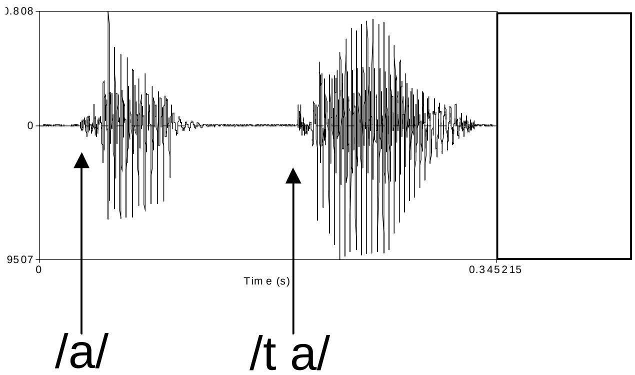


**Figure 1.** Example of the *'atta'* stimulus, showing it's time course and frequency spectra.

*2.4. Temporospatial PCA*

For the averaged ERP and CSD waveforms a temporospatial PCA was applied. In other words, first a temporal, then a spatial PCA were conducted to avoid the conflation of different ERP components with similar time courses. As a rotation method for both - temporal and spatial – PCA, a Varimax rotation with 99% extraction criteria was used (Kayser & Tenke, 2003; Beauducel & Debener, 2003; van Boxtel, 1998). Thus, extracted components accounting for 99 % of the variance were rotated. A covariance matrix was chosen based on the recommendations made by Kayser & Tenke (2003) and Dien et al. (2005).

In order to find the time points which vary most across participants and experimental conditions, 685 sample points (-300 – 1068 ms) as variables and 15480(ERP)/9720(CSD) observations (participants x condition (i.e. oddball and EQ)/stimuli (i.e. standard *'atta'*, deviant *'atta'*, deviant *'appa'* and EQ *'atta'* and *'appa'*) x electrode sites) were submitted to the temporal PCA. A set of principal components, virtual epochs, were thereby extracted.

Next, temporal components for the succeeding spatial PCA were selected, if their factor loadings and topographies (spatial configurations) resembled real ERP components. Consequently, the selection was not strictly restricted to the studied negative obligatory ERP components at this point, because it was assumed that the following spatial PCA would benefit also from the variance of other components (e.g. P1, P2) or even noise-related variance at the time range at which the N1 and N250 were observed in the grand average waveforms (Kayser & Tenke, 2003).

Accordingly, the temporal factor scores from the chosen components were rearranged so that the scores for each observation were positioned as variables. The reconstructed dataset was then subjected to the spatial PCA (685 time points as observations). The obtained components were, correspondingly, referred to as virtual electrodes (see Results for more detailed description).

*2.5. Statistical analyses for the selected PCA factor scores*

The selection of the spatial components (virtual electrodes) for the statistical analyses was made based on the topographic distributions and aggregated factor scores of the spatial PCA components. Each selected spatial ERP- and CSD-PCA component was examined in relation to the temporal PCA components active at the latency of the studied ERP components.

Spatial components active at the latency of ~100 ms and with frontal or frontocentral scalp distribution were thought to resemble N1b and components with a distribution maximal posterior to that of N1b were assumed to reflect non-specific N1 activity. Additionally, spatial components active at ~ 45 ms after N1 with a temporal distribution were regarded as Tb of the T-complex. Furthermore, the factor scores of the components at the latency of N1 activity were assumed to be dominated by the *long ISI condition*. Considering the N250, spatial components active at the latency of ~250 ms with a frontal or frontocentral distribution were examined. The factor scores of these components were assumed to be almost equally active in *short* and *long ISI conditions*, because N250 has been shown to be insensitive to ISI changes (Ceponiene et al., 1998, 2002). Statistical analyses were restricted to the comparison of standard *'atta'* stimuli (i.e. /s8dt-satta/ and /s8dp-satta/) from the *short ISI condition* with the *'atta'* stimulus (i.e. /ata8-datta8/) in the *long ISI condition*[1]. To find out if there were significant differences between the *short* and *long ISI conditions*, the factor scores of the selected components were submitted to separate paired-samples T-tests for both conditions. A conventional significance level ($p<0.05$) was applied.

The factor scores of ERP- and CSD-PCA are not directly proportional. Consequently, no statistical analyses were performed to compare the selected spatial components extracted by the two methods. Instead, a descriptive comparison of the topographic distributions and spatial factor scores of the selected components was conducted (see Discussion).

## 3. Results

### *3.1. Average ERP and CSD waveforms*

Grand average event-related potential (ERP) waveforms of the surface potentials and the scalp topography maps at the peak latencies of N1 and N250 are shown in Fig. 2, separately for *short* and *long ISI conditions*. When it comes to the investigated ERP components, in the *short ISI condition* a small negativity was observable at 118 ms, which was not, however, visible in the topography map. The small negativity was followed by a large frontocentrally maximal negativity peaking at 260 ms, representing N250. In the *long ISI condition*, a clear N1 component was identified at 110 ms, succeeded by a N250 at 290 ms. In the topography maps, a central-posterior negativity for the N1 and a frontocentral negativity for the N250 were observed.

[1] To avoid needless complexity, the factor scores of the two standard *'atta'* stimuli were aggregated as one variable representing the *short ISI condition*, and compared with the *'atta'* stimulus from the *long ISI condition*.

The reference-free current source density (CSD) transformations of the ERP waveforms, and the scalp topography maps at the peak latencies of N1 and N250, are shown in Fig. 3. In the *short ISI condition*, a small negativity was barely observable at 104 ms. In the scalp topography, small frontal and posterior negativities were visible, but positivity was predominating. A large frontocentral negativity was evident at 260 ms, representing N250. In the *long ISI condition*, a clear central-posterior negativity was observable at 104 ms, followed by a central negativity at 288 ms, representing N1 and N250, respectively. The scalp topographies of the *long ISI condition* were much alike, but at N1 latency, a posterior negativity predominated, whereas at N250 latency, a central negativity was grater. Altogether, in line with theoretical assumptions, the topographies of N250 in both conditions for ERP and CSD waveforms were noticeably similar, whereas the topographies at N1 latency differed considerably.

### *3.2. Temporospatial PCA of ERP and CSD waveforms*

The analysis began by submitting both, ERP and CSD, data to a temporal PCA. In total, 57 components in the ERP data and 73 in the CSD data, respectively, were acquired to sufficiently explain 99% of the data sets. By visual inspection, the time courses of CSD factor loadings seemed sharper and more distinct than those of ERP data. Moreover, a larger amount of CSD-PCA factors were acquired to explain the data, compared to the ERP-PCA solution. Both PCA solutions, however, resembled closely each other. The only marked exception was the double-peaked component T1-282-454-608, accounting for 51,2 % of the ERP data, corresponding to the two distinct T3-286 and T2-614 factors, together accounting for 17,7 % of the CSD data.

For the subsequent spatial PCA, ten temporal components from the ERP data (Figs. 4 and 5) and fourteen components from the CSD data (Figs. 6 and 7) were selected on the account of their temporal and topographical characteristics. Consequently, components were selected, if their factor loadings peaked at 76-500 ms for the ERP data and at 70-420 ms for the CSD data, respectively. The time range criterion for the factor loadings was determined by utilizing the information about real ERP component latencies (N1, N250) in the grand averages. Moreover, loadings of the factors had to reach the 0.7/0.07 (ERP/CSD) criterion for at least one time point. In addition, the topographies (spatial configurations) of the selected components resembled real ERP components.

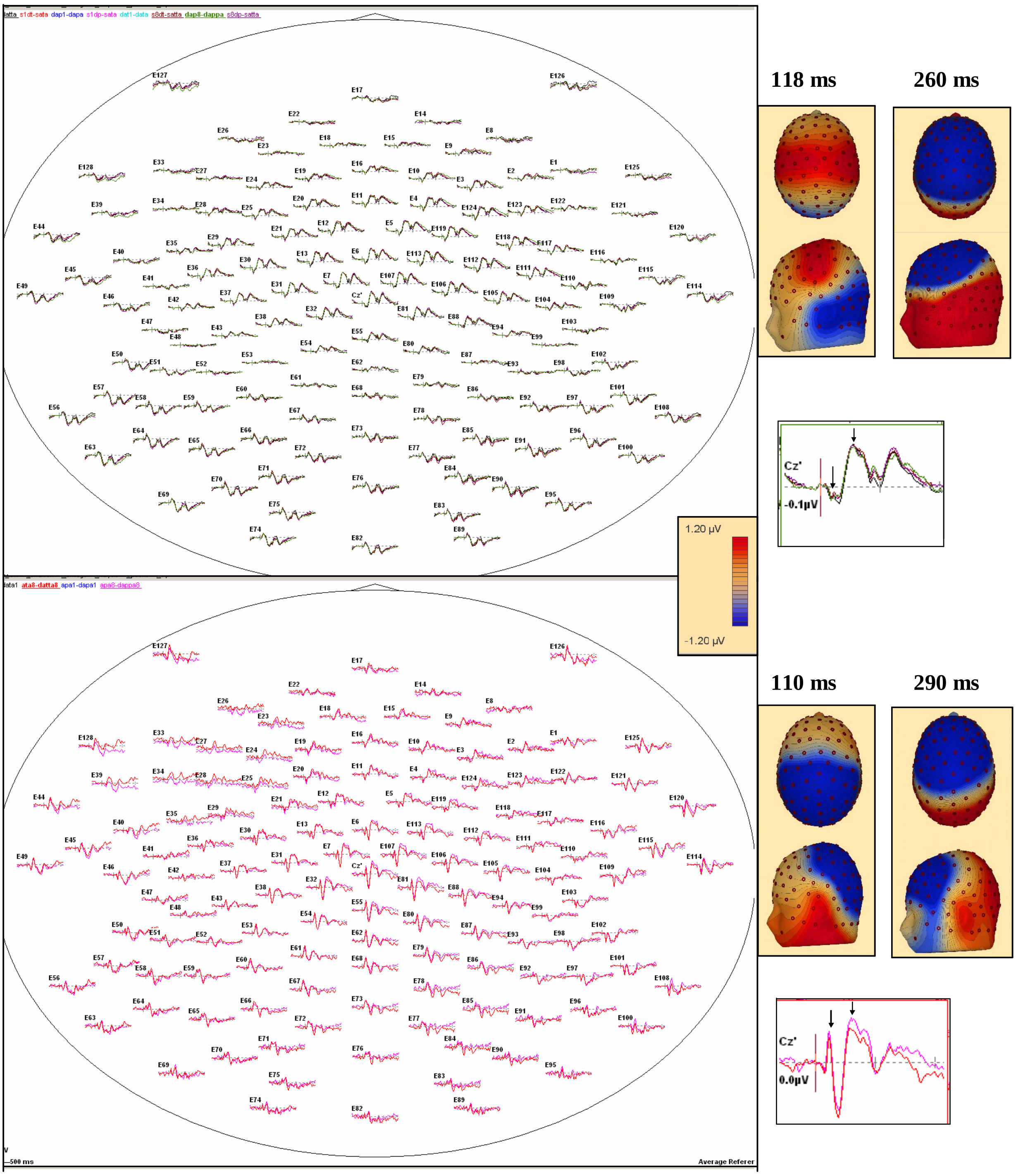


**Figure 2.** Left: Grand average event-related potential (ERP) waveforms for 20 healthy children at all 129 electrodes. Upper figure includes responses of the *short ISI condition* stimuli (oddball) *'dat8-datta'*, *'s8dt-satta'*, *'dap8-dappa'* and *'s8dp-satta'*. Lower figure includes responses of the *long ISI condition* (EQ) stimuli *'ata8-datta8'* and *'apa8-dappa8'*. Right: Scalp topographies of the grand averages at the peak latencies of N1 and N250, separately for *short* (up) and *long ISI* (below) stimuli.

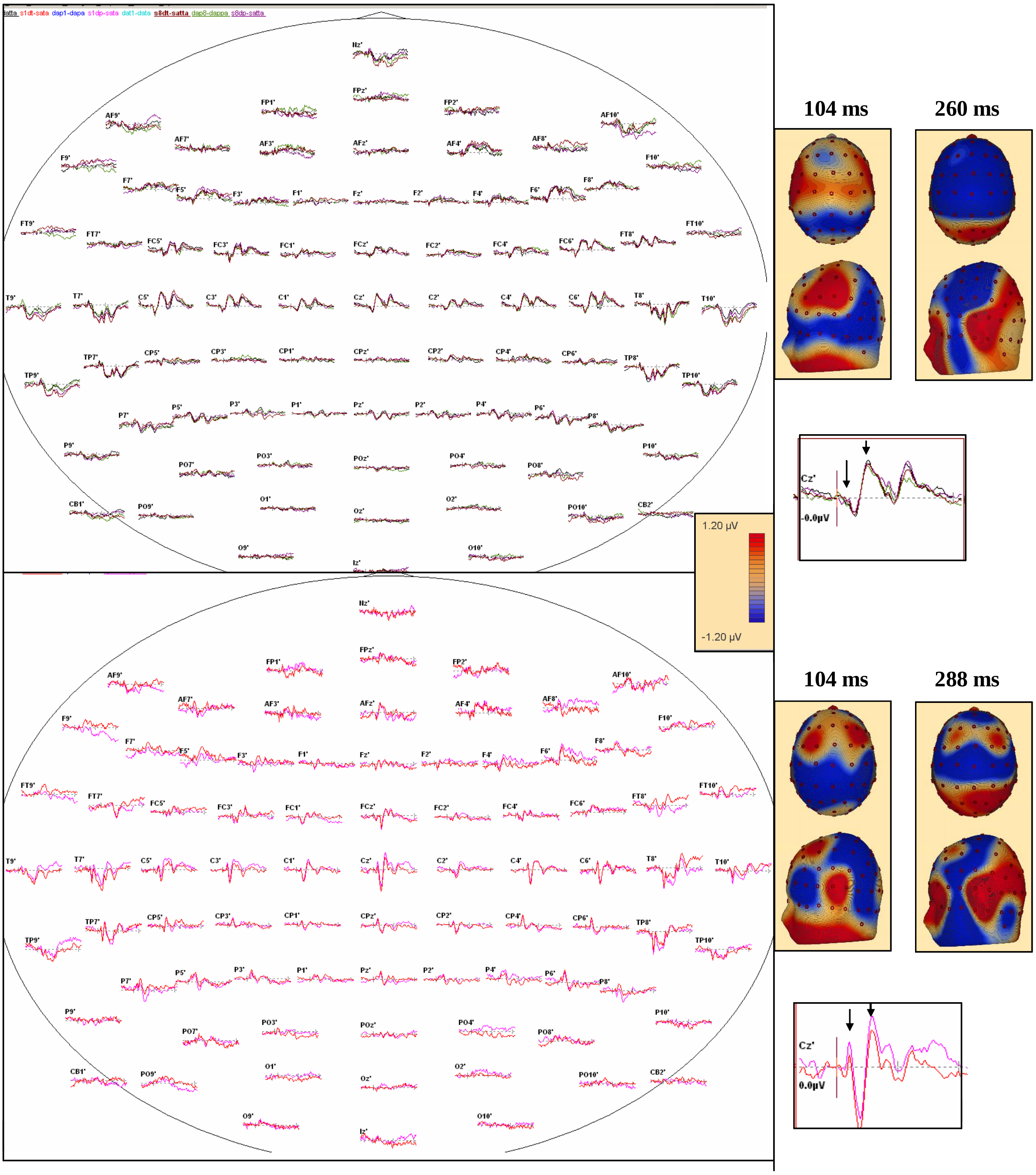


**Figure 3.** Left: Reference-free current source density (CSD) waveforms for 20 healthy children at all 129 electrodes. Upper figure includes responses of the *short ISI condition* (oddball) stimuli *'dat8-datta'*, *'s8dt-satta'*, *'dap8-dappa'* and *'s8dp-satta'*. Lower figure includes responses of the *long ISI condition* (EQ) stimuli *'ata8-datta8'* and *'apa8-dappa8'*. Right: Scalp topographies of the CSD waveforms at the peak latencies of N1 and N250, separately for *short* (up) and *long ISI* (below) stimuli.

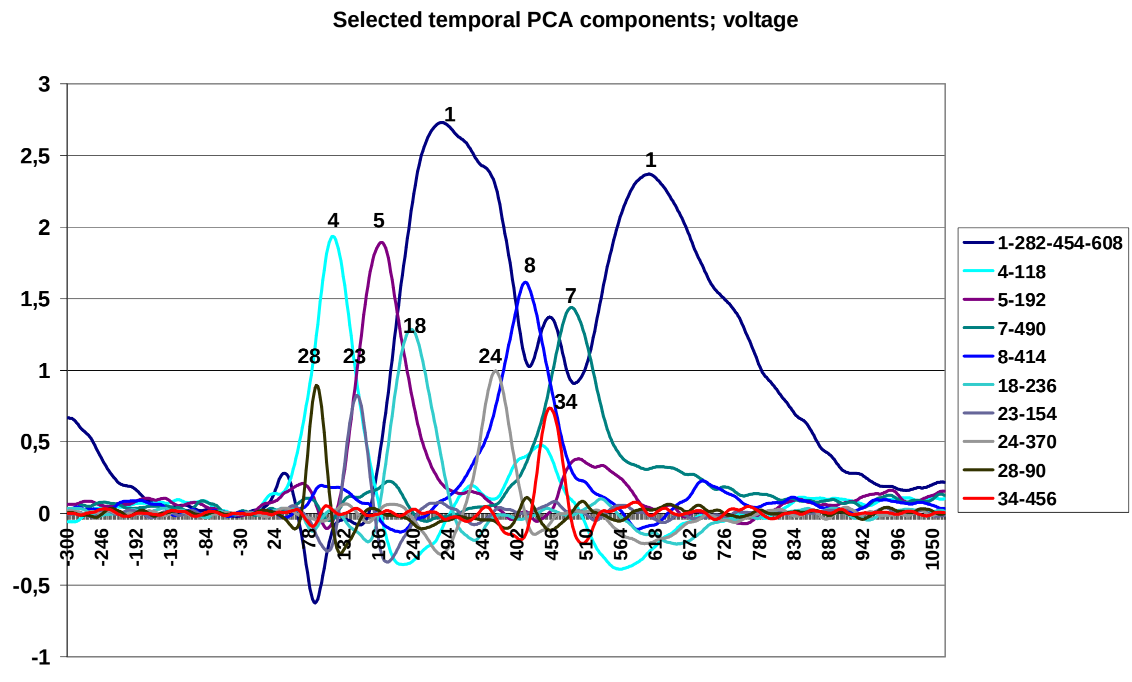


**Figure 4.** The selected ten temporal factor loadings extracted from ERP waveforms. The peak latency and the number of each component are shown in the box (right).

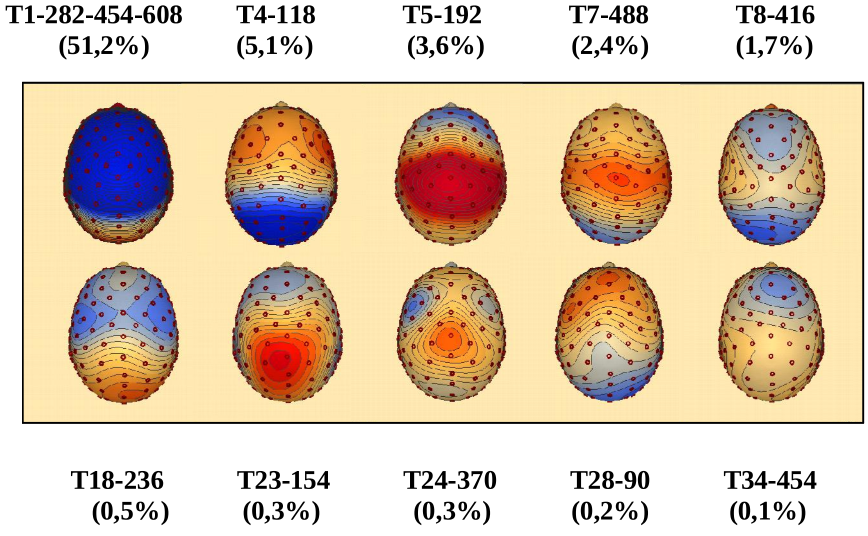


**Figure 5.** The selected ten temporal factor score topographies extracted from ERP waveforms. Percentage of the variance accounted for by each component after rotation is shown in parentheses.

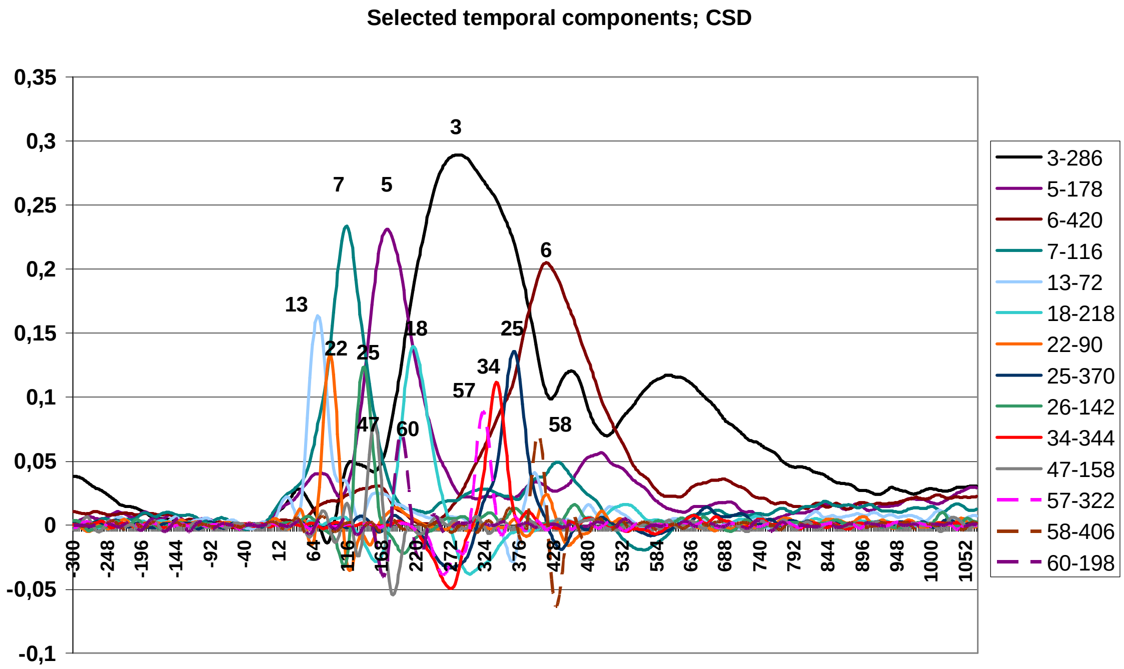


**Figure 6.** Selected fourteen temporal factor loadings extracted from CSD waveforms. The peak latency and the number of each component is shown in the box (right).

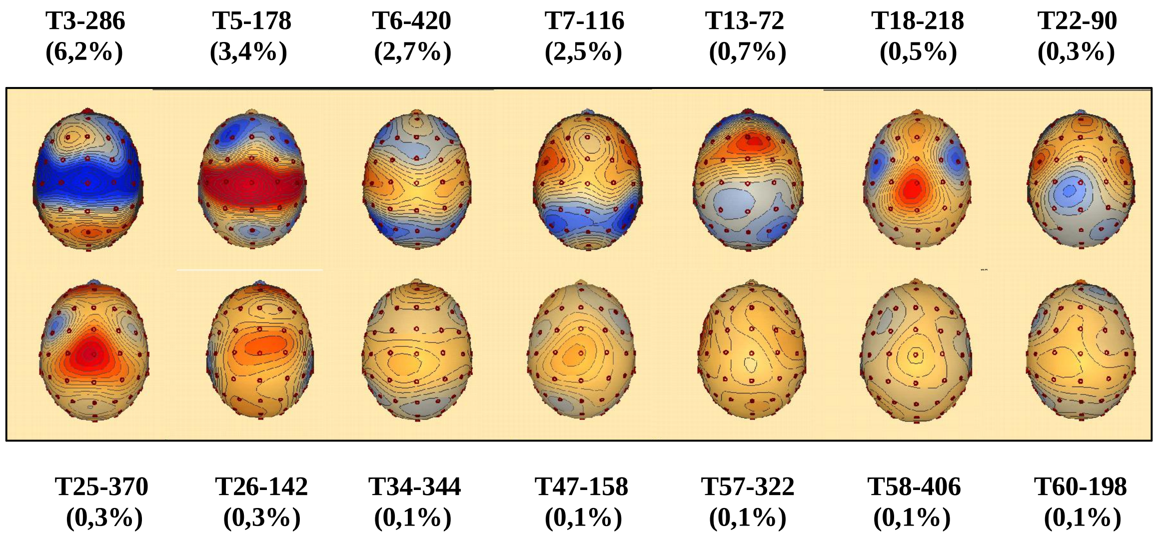


**Figure 7.** The selected fourteen temporal factor score topographies extracted from CSD waveforms. Percentage of the variance accounted for by each component after rotation is shown in parentheses.

The selected temporal components (from both data sets separately) were then submitted to spatial PCA. A total of 80 spatial components in the ERP data and 64 in the CSD data accounted for 99 % of the data sets. The first fifteen spatial components from both data sets are shown in Fig. 8. The selection of spatial components for statistical analyses was made among these fifteen components. Note, that the spatial factor score topographies represent the *common variance* between spatial component and the temporal components, and are not directly comparable to ERP and CSD maps.

**Spatial ERP-PCA components** **Spatial CSD-PCA components**

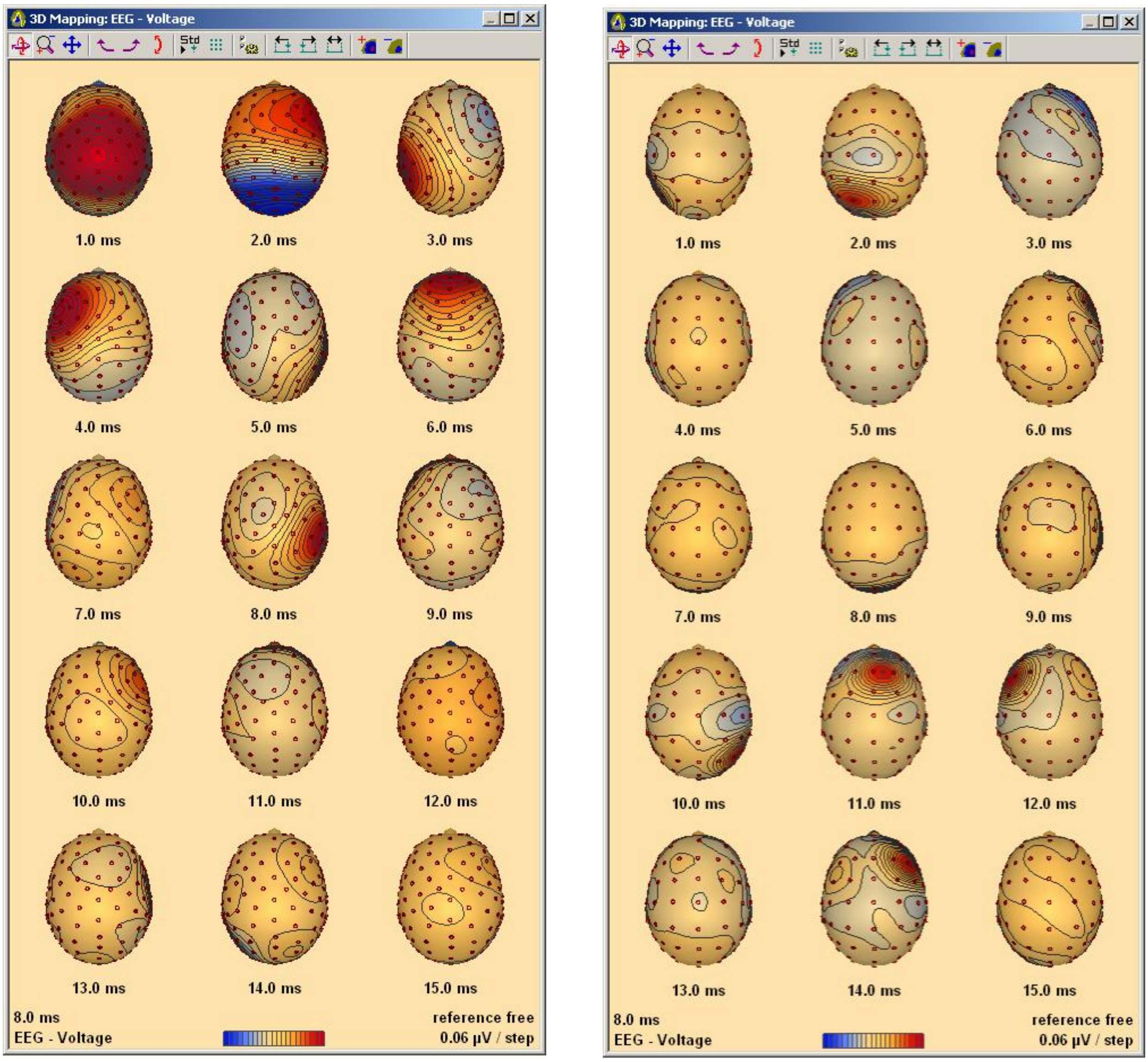


**Figure 8.** The first fifteen spatial ERP- and CSD-PCA components extracted from the selected temporal PCA components.

*3.3. Statistical results of the selected temporospatial PCA factor scores*

The selection of the obtained spatial components for the statistical analysis was restricted to the components that could be related to the investigated ERP components through their temporal and spatial characteristics. Moreover, only components with large and representative PCA factor scores, at the latencies of the investigated ERP components, were selected for further analysis. Thus, the most active spatial components at the latencies (i.e. virtual epochs) of the investigated ERP components – indicated by the factor scores – were studied further. All the selected components (factor scores and topographies) are shown in Figs. 9.-10., separately for ERP and CSD data.

*3.3.1. ERP-PCA*

*N1 components.* Spatial component S4 had a frontal scalp distribution and large factor scores at the latency of N1b (i.e. T4-118). The factor scores of S4-T4 were positive, indicating frontal positivity. No statistical differences between the *short* and *long ISI conditions* were found ($t$ (19) = -1.262, $p$ = .222), although the factor scores were dominated by the *short ISI condition* by visual inspection.

Spatial component S2 was maximal posterior to the scalp distribution of N1b and was active at the latency of non-specific N1 component (i.e. T4-118). The factor scores of S2-T4 were positive, indicating posterior negativity, and slightly dominated by the *short ISI condition*. No statistical differences between conditions were found ($t$ (19) = .092, $p$ = .928).

Spatial components S3 and S5 had a temporal distribution and large factor scores at the latency of Tb (i.e. T23-154). The factor scores of S3-T23 and S5-T23 were negative, indicating negativities on the left (i.e. S3-T23) and right (i.e. S5-T23) temporal lobes. The conditions were almost equally active for S3-T23, whereas the *short ISI condition* slightly dominated the factor scores of S5-T23. Comparisons of conditions did not reach statistical significances (S3-T23: $t$ (19) = -.080, $p$ = .937; S5-T23: $t$ (19) = .540, $p$ = .595).

*N250 components.* Spatial components S1 and S2 had a central and frontal distribution and were active at the latency of N250 (i.e. T1-282-454-608). The factor scores of S1-T1 were negative, indicating central negativity. For S2-T1 the factor scores were negative, indicating frontal negativity. The factor scores of the components were almost equally active and, accordingly, no significant differences between conditions were found (S1: $t$ (19) = .301, $p$ = .767; S2: $t$ (19) = .015, $p$ = .988).

*3.3.2. CSD-PCA*

*N1 components.* Spatial components S12 and S14 had a frontocentral scalp distributions and large factor scores at the latency of N1b (i.e. T7-116). The factor scores of S12-T7 were dominated by the *short ISI condition*, while the opposite was true for S14-T7. Factor scores of both components were positive, indicating frontal sources on left (i.e. S12-T7) and right (i.e. S14-T7) hemispheres, accompanied with anterior sinks. For S12-T7, significant differences between *short and long ISI conditions* were found ($t$ (19) = -2.290, $p$ = .034), indicating sensitivity to ISI changes. The factor scores of S14-T7 did not differ significantly between conditions ($t$ (19) = .767, $p$ = .452).

Spatial component S2 was maximal posterior to the scalp distribution of N1b and was active at the latency of non-specific N1 component (i.e. T7-116). The factor scores of S2-T7 were negative in the *short* and positive in the *long ISI condition*, indicating a posterior sink in the *short ISI condition* and a central sink in the *long ISI condition*. The comparison of the factor scores did not reach statistical significance ($t$ (19) = -1.031, $p$ = .315), but the opposite weightings of the factor scores indicate a shift in the topographical distribution due to ISI change.

Spatial components S4 and S13 had temporal distributions and large factor scores at the latency of Tb (i.e. T26-142). The factor scores of S4-T26 were positive in the *short* and slightly negative in the *long ISI condition*. The difference between conditions was not significant ($t$ (19) = 1.024, $p$ = .319), indicating a left temporal source. The factor scores of S13-T26 were positive for both conditions, and dominated by the *short ISI condition*, indicating a right temporal source. No significant differences were found between conditions ($t$ (19) = 1.274, $p$ = .218).

*N250 components.* Spatial components S6, S4 and S13 had a frontal or *temporal*[2] scalp distributions and large factor scores at the latency of N250 (i.e. T3-286). The factor scores of S6-T3 were negative and dominated by the *long ISI condition*, indicating a lateral frontal sink. Differences between conditions were significant ($t$ (19) = 2.669, $p$ = .015), indicating sensitivity to ISI changes. Factor scores of S4-T3 and S13-T3 were positive, indicating temporal sources on both hemispheres. For S4-T3, the factor scores were dominated by the long *ISI condition*, while the opposite was true for S13-T3. No significant differences were found between the *short* and *long ISI conditions* of these two components (S4-T3: $t$ (19) = -.339, $p$ = .738; S13-T3: $t$ (19) = .848, $p$ = .407).

[2] Although not frontally or frontocentrally maximal, components S4 and S13 were thought to represent N250 activity because of their considerably large spatial factor scores at the latency of N250 (i.e. T3-286; Fig. 10).

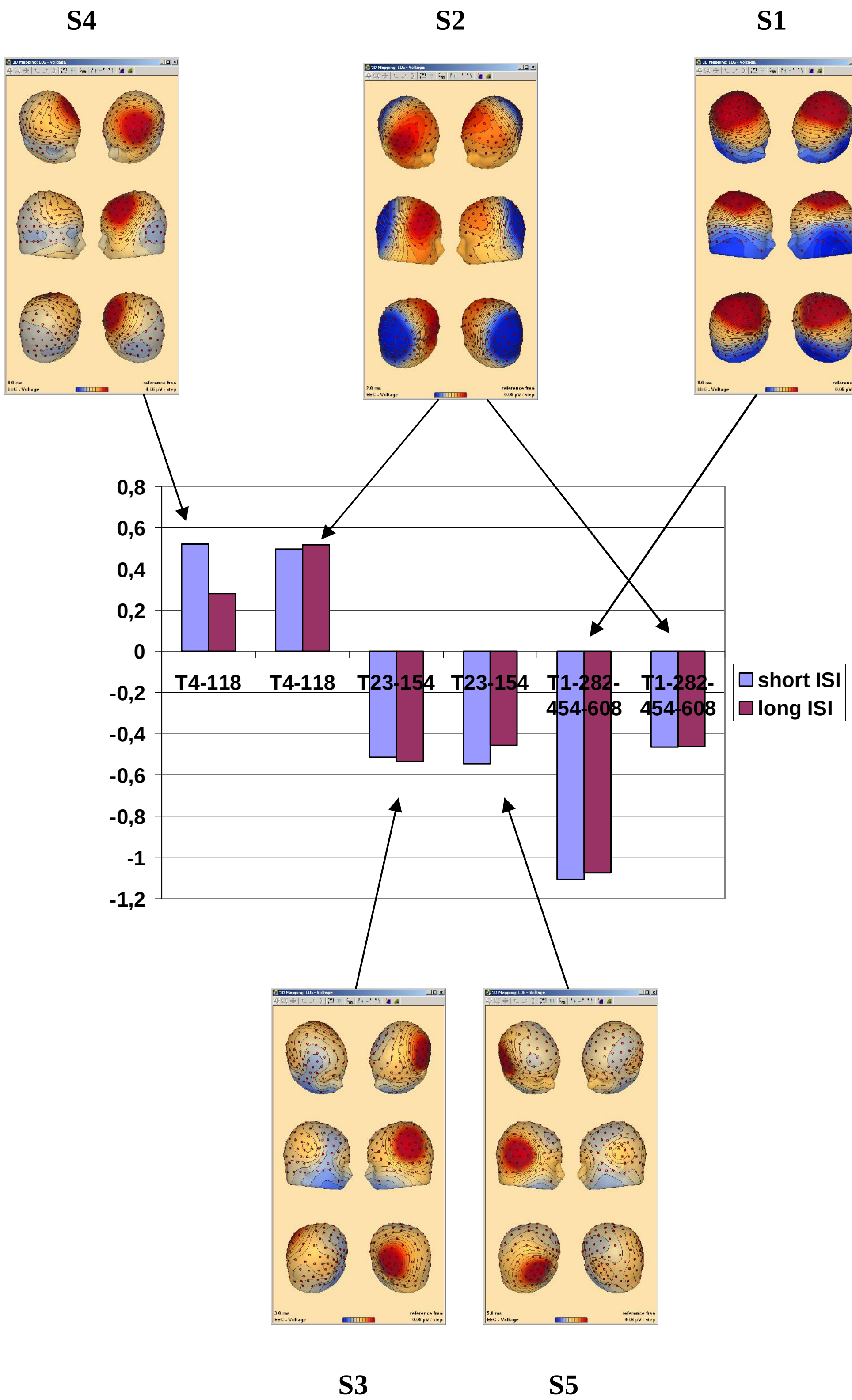


**Figure 9.** The scalp topographies and factor scores (including stimuli */s8dt-satta/*, */s8dp-satta/* and */ata8-datta8/*) of the selected spatial ERP-PCA components in relation to the temporal ERP-PCA components active at the latency of the studied ERP components.

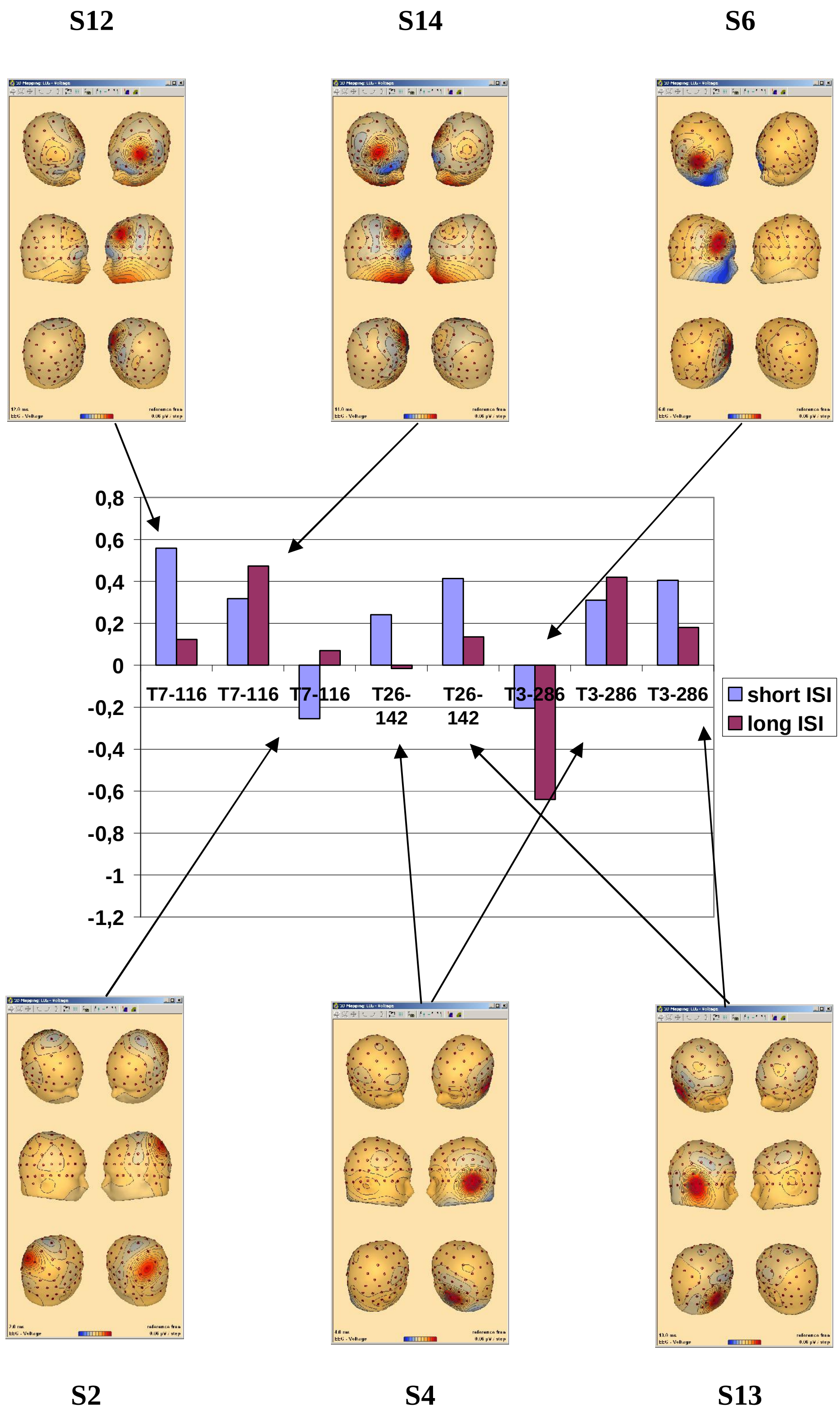


**Figure 10.** The scalp topographies and factor scores (including stimuli */s8dt-satta/*, */s8dp-satta/* and */ata8-datta8/*) of the selected spatial CSD-PCA components in relation to the temporal CSD-PCA components active at the latency of the studied ERP components.

## 4. Discussion

The purpose of this study was to explore if principal component analysis (PCA) was an efficient and reliable method for extracting temporally and spatially close or overlapping ERP components measured with dense electrode array. This was done by evaluating and comparing the ability of two different solutions within temporospatial PCA – ERP-PCA and CSD-PCA – to separate auditory N1 and N250 from each other. Both PCA solutions were expected to be able to extract the desired components, although CSD-PCA was assumed to surpass the more traditional ERP-PCA in accuracy. The data was obtained from 9-year-old children by auditory oddball and EQ (control) paradigms with the inter-stimulus-intervals of 610 ms in the oddball and 1-5 s in the EQ paradigm. The stimuli from the oddball paradigm were jointly referred to as the *short ISI condition*, whereas the stimuli from the EQ paradigm, respectively, as the *long ISI condition*. Consequently, temporospatial PCA components thought to represent N1 activity were assumed to differ between conditions, whereas the conditions of N250 components were assumed not to differ (Ceponiené et al., 1998, 2002). The topographical configurations of the extracted spatial PCA components (i.e. virtual electrodes) were assumed to have negative scalp distributions either frontally, centrally or temporally, depending on the ERP component it was assumed to represent. Furthermore, the factor scores of the selected spatial PCA components had to be large and representative at the latency (i.e. virtual epoch) of the investigated ERP components.

As expected, the temporal PCA factor loadings derived from ERP and CSD data (Figs. 4 and 6) resembled closely each other, although there were less overlap among the CSD factor loadings. The spatial factor scores and topographies (Figs. 8, 9 and 10), however, differed considerably between the two solutions, the CSD-PCA scores and topographies being sharper and more distinct. Both PCA solutions extracted components that were associated with N1 subcomponents, as well as N250. Moreover, the components extracted by CSD-PCA solution were more focal and easier to associate with real ERP components than the topographically more extensive components extracted by ERP-PCA solution.

Using a two-step PCA as a method for analyzing high-density ERP data was found to be confirmative as well as informative. Moreover, it considerably reduced the amount of information obtained by the 129 electrodes, facilitating the selection of physiologically relevant components for further analysis. Temporospatial PCA was able to disentangle spatial distributions visible in the real ERP grand averages. In addition, it certainly has the ability to extract ERP subcomponents not visible in the grand averages, but the interpretation of such components should be carried out with caution. Unfortunately temporospatial PCA loses the information about the channels and no critical examinations about or comparisons between their contributions can be made (Kayser & Tenke, 2006a). On the other hand, the aim of this study was to analyse multi-channel ERP data in an all-inclusive fashion, not merely in relation to certain selected channels. It was concluded that a two-step PCA suits well especially for the purposes of explorative analysis of high-density ERP data. An explorative analysis is ideal for maturational ERP data, because no consensus of children's ERP maturation processes or component structures has been achieved (e.g. Johnstone et al., 1996; Ceponiené et al., 1998; Gomes et al., 2001). In this study the assumption was, according to Johnstone et al. (1996) that ERP components N1 and N250 correspond to those of adults' N1 and N2. There is, however, no certainty about the correspondence of adult ERP components to those of children (Albrecht et al., 2000).

The association of the extracted temporospatial PCA components to real N1 and N250 activity was rather easy when they were directly proportional to the topographies of the grand average ERP and CSD waveforms. However, as far as ERP subcomponents – not visible in the grand average – are concerned, it is very difficult to prove that the selected spatial PCA components actually represent certain ERP subcomponents. Here, this problem was attempted to overcome by utilizing the theoretical information about the effects of *short* and *long ISI* experimental conditions on the ERP components of children (Karhu et al., 1997; Gomes et al., 2001; Ceponiené et al., 1998, 2002).

### *4.1. Selected temporospatial PCA components associated with real ERP components*

#### *4.1.1. ERP-PCA*

For the ERP-PCA (Fig. 9), no evidence of sensitivity to ISI changes was found among the chosen components associated with N1 activity. In addition, component S4-T4, thought to represent N1b, was frontally positive indicated by the factor scores. It is therefore unlikely that the component in question actually reflected N1b activity. Component S2-T4, associated with the non-specific N1, had a negative scalp distribution posterior to vertex and was almost equally active in both, *short* and *long ISI*, conditions. This would imply that the non-specific N1 component is observable also with short ISIs in children. According to the weighing of the factor scores, components S3-T23 and S5-T23 had a temporally negative topography, indicating Tb of T-complex – separately for both hemispheres. Judging from the fact that the factor scores of the components were almost equally active in both conditions, it would support the conclusions of Gomes et al. (2001) that T-complex is observable from early childhood even with short ISIs. There were two components associated with N250; S1-T1 indicating central and S2-T1 frontal negativity. In line with the assumptions (Ceponiené et al., 1998, 2002), N250 seemed to be insensitive to ISI changes.

*4.1.2. CSD-PCA*

For the CSD-PCA (Fig. 10), evidence of ISI sensitivity was found for S12-T7 component, thought to represent the left dipole of N1b. The factor scores of this component were positive and dominated by the *short ISI condition*, indicating a frontal positivity and a slightly weaker negativity anterior to it. The same was true for S14-T7 assumed to reflect the right dipole of N1b, except for the evidence of ISI sensitivity. Thus, this would imply that it is improbable for these components to reflect N1b activity, because the predominance of the negativity associated with N1b shifts from anterior to more central after age 6 (Ceponiené et al., 2002). The factor scores of the component S2-T7, associated with the non-specific N1, were negative in the *short ISI condition* and positive in the *long ISI* condition, indicating a posterior negativity in the *short ISI condition* and a central negativity in the *long ISI condition*. Although the difference was not significant, it could be inferred that the non-specific N1 component was observable in both conditions, and its topography was affected by changes in the inter-stimulus-interval. This would be logical, because all the other N1 subcomponents are sensitive to ISI changes (Ceponiené et al., 1998, 2002). According to the previous research, however, the shift of the negativity has been from central to posterior with longer ISIs (Näätänen & Picton, 1987; Ceponiené et al., 2002). In that sense this result is contradictory to the previous findings. As for the components reflecting Tb (i.e. S4-T26 and S13-T26), it appeared that these temporally maximal components were observable even with short ISIs, supporting the suggestion of Gomes et al. (2001). Interestingly, the topographies of these two components were temporally positive, indicated by the factor scores. A positive peak at temporal sites called Ta, which is a predecessor of the negativity (Tb) in the T-complex, is usually elicited at the peak latency of N1 (e.g. Ponton et al., 2000; Tonnquist-Uhlen et al., 2003). The frontally negative component S6-T3, as well as the *temporally* positive components S4-T3 and S13-T3, were assumed to represent N250 activity. Contrary to the previous research (Ceponiené et al., 1998, 2002), the frontal component seemed to be sensitive to ISI changes. The temporally positive components speak in favour of Ta-like radially oriented subcomponents, active in conjunction with N250.

*4.1.3. Comparison of the selected ERP- and CSD-PCA components*

Due to the fact that ERP-PCA and CSD-PCA are not directly proportional, only descriptive and suggestive comparisons can be made. It is clear that despite of certain similarities, the outcomes of these two solutions on the same data set were somewhat different. What can be inferred, however, is that neither of the solutions could extract a clear component reflecting N1b. Children's N1 has been reported to be either frontal (e.g. Johnstone et al., 1996; Ceponiené et al., 2002) or frontocentral (e.g. Ceponiené et al., 1998, 2001; Ponton et al., 2000), but the weighing of N1 subcomponents in the scalp distribution is still unclear. In the grand averages of this study, only negativities posterior to vertex were visible at the latencies of N1, indicating non-specific N1 component. In fact, non-specific N1 was extracted by both of the PCA solutions, with short and long ISIs. It is possible that the more robust non-specific N1 superimposed N1b and the consequent temporal and spatial overlap was too challenging for PCA. The non-specific N1 has been concluded to be an orienting component with a long refractory period (Näätänen & Picton, 1987; Ceponiené et al., 1998). Thus, in an averaged data it can distort the magnitude of the simultaneously occurring N1b component, which is not necessarily even visible in the grand averages. When it comes to the negative peak of the T-complex (Tb), there was clear activation at temporal leads at the latency of Tb in both data sets. In the CSD-PCA data, however, the activation was positive indicating Ta, which is usually elicited in conjunction with N1. Yet, it is not unquestionable that this activation was a manifestation of Ta, because it was maximal ~ 40 ms after N1 peak visible in the grand average. Accordingly, the possibility exists that T-complex represents the inversion of the N1, but there is also evidence of its independence (Ponton et al., 2002; Tonnquist-Uhlen et al., 2003). In other words, if the activation in question would not depend on the latency of N1, it could in fact represent Ta activity. Altogether, these results support the suggestion of Tonnquist-Uhlen et al. (2003) that T-complex components are observable in children even with short ISIs (see also Karhu et al., 1997; Ceponiené et al., 1998; Gomes et al., 2001). For the components representing N250, the common feature between solutions was a frontal negativity. It could, however, be argued that in the CSD-PCA data, the frontal component did not represent N250 because of its sensitivity to ISI changes (Ceponiené et al., 1998, 2002). On the other hand, in the studies of Ceponiené et al. (1998, 2002) the amount of subjects and recording channels was relatively small and could have resulted in false conclusions about the properties of N250. Interestingly, in the CSD-PCA data, Ta-like positive peaks at temporal sites were additionally observed, which suggests that N250 might also have radial subcomponents (cf. N1, P1; e.g. Karhu et al., 1997; Albrecht et al., 2000). The robust central N250 component S1-T1 of ERP-PCA data, not visible in the CSD-PCA data, could have been a result of the distorting effect of the extensive temporal component T1 ranging from 282 ms to 608 ms.

As can be inferred from these results, the hypothesis that PCA would separate ERP components specific to the *short* and *long ISI conditions* was not fully verified. The two N1 subcomponents extracted by PCA did not consistently differ as a result of the changes in ISIs. The differences between *short* and *long ISI conditions* were obvious in the grand averages of ERP and CSD data, but PCA was not able to disclose them as expected. However, they were better brought out by CSD-PCA. It is possible that PCA misallocated the variance in the data and, thus, emphasized the activation of *short* and *long ISI conditions* incorrectly. Additionally, ERP data collected from children subjects has considerably lower signal-to-noise-ratio and a higher risk for latency jitter than a data collected from adults. Also the age of the children subjects used in this study is critical in a way that around age 9, developmental changes in the brain start to occur and marked individual differences in the measured event-related potentials are likely (e.g. Johnstone et al., 1996; Ponton et al., 2000). However, PCA could have interpreted the N1 and N250 components in both conditions as reflecting the same processes and, thus, did not separate them as distinct components.

### *4.2. Conclusions*

It was made clear by this study that different methodological approaches can have substantial effects on the interpretations made about ERP components. In line with previous studies by Kayser & Tenke (2006a, 2006b) and Kayser et al. (2006), the results support the use of CSD-PCA in the analysis of multi-channel ERP data. It seems that ERP-PCA reveals the overall activation of the data, whereas CSD-PCA enables more detailed and exact summary about the distribution of the variance. Furthermore, a two-step PCA was concluded to be an ideal method for an explorative analysis of ERP data. From a methodological point of view, a challenge for future research is to study and compare the ability of two-step ERP-PCA and CSD-PCA to extract ERP components with a data collected from adult subjects. While real ERP data is crucial when validating new ERP analyzing methods, simulation studies could give additional information about their strengths and weaknesses.

The development of ERP recording and measuring equipment preconceives that ERP analyzing methods develop as well. New methods, such as principal component analysis and independent component analysis (e.g. Hyvärinen & Oja, 2000; Makeig, Debener, Onton, & Delorme, 2004), enable more distinct and comprehensive picture about the features of ERP data. Although the purpose of component analyses is to efficiently summarize the information of ERP data set, they yet extract vast amounts of components from which the relevant ones ought to be selected. Thus, the problem of the disputed association between PCA components and ERP components still remains. In future research, the selection of components could be facilitated by combining PCA technique with dipole source localization procedure (Dien et al., 2003). Nevertheless, the development of ERP analysing methods is not likely to eliminate or even diminish the demand for the researchers’ extensive knowledge about the physiology of ERP components.

## References


Albrecht, R., von Suchodoletz, W., Uwer, R. (2000). The development of auditory evoked dipole source activity from childhood to adulthood. *Clinical Neurophysiology*, 111, 2268-2276.

Beauducel, A., & Debener, S. (2003). Misallocation of variance in event-related potentials: simulation studies on the effects of test power, topography, and baseline-to-peak versus principal component quantifications. *Journal of Neuroscience Methods*, 124, 103-112.

Bishop, D. W. M., Hardiman, M., Uwer, R., von Suchodoletz, W. (2007). Maturation of the long-latency auditory ERP: step function changes at start and end of adolescence. *Developmental Science*, 10, 565-575.

Boxtel, G. J. M. van (1998). Computational and statistical methods for analysing event-related potential data. *Behavior Research Methods, Instruments, & Computers*, 30, 87-102.

Casarotto, S., Bianchi, A. M., Cerutti, S., Chiarenza, G. A. (2004). Principal component analysis for reduction of ocular artefacts in event-related potentials of normal and dyslexic children. *Clinical Neurophysiology*, 115, 609-619.

Ceponiené, R., Cheour, M., Näätänen, R. (1998). Interstimulus interval and event-related potentials in children: evidence for multiple generators, *Electroencephalography and Clinical Neurophysiology*, 108, 345-354.

Ceponiené, R., Shestakova, A., Balan, P., Alku, P., Yianguchi, K., Näätänen, R. (2001). Children's auditory event-related potentials index sound complexity and "speechness". *International Journal of Neuroscience*, 109, 245-260.

Ceponiené, R., Rinne, T., Näätänen, R. (2002). Maturation of cortical sound processing as indexed by event-related potentials. *Clinical Neurophysiology*, 113, 870-882.

Ceponiené, R., Alku, P., Westerfield, M., Torki, M., Townsend, J. (2005). ERPs differentiate syllable and non-phonetic sound processing in children and adults. *Psychophysiology*, 42, 391-406.

Chapman, R. M., & McCrary, J. W. (1995). EP component identification and measurement by principal components analysis. *Brain and Cognition*, 27, 288-310.

DeFrance, J. F., Sands, S., Schweitzer, F. C., Gingsberg, L., Sharma, J. C. (1997). Age-related changes in cognitive ERPs of attenuation. *Brain Topography*, 9, 283-293.

Delorme, A., & Makeig, S. (2004). EEGLAB: an open source toolbox for analysis of single-trial EEG dynamics including independent component analysis. *Journal of Neuroscience Methods*, 134, 9-21.

Delplanque, S., Silvert, L., Hot, P., Sequeira, H. (2005). Event-related P3a and P3b in response to unpredictable emotional stimuli. *Biological Psychology*, 68, 107-120.

Dien, J., Spencer, K. M., Donchin, E. (2003). Localization of the event-related novelty response as defined by principal component analysis. *Cognitive Brain Research*, 17, 637-650.

Dien, J., Beal, D. J., Berg, P. (2005). Optimizing principal component analysis of event-related potentials: Matrix type, factor loading weighting, extraction, and rotations. *Clinical Neurophysiology,* 116, 1808-1825.

Dien, J., & Frishkoff, G. A. (2005). Principal components analysis of event-related potential datasets. In Handy, T. (Ed.), *Event-related potentials: a methods handbook.* Cambridge, MA: MIT Press.

Donchin, E., Ritter, W., & McCallum, W. C. (1987). Multivariate analysis of event-related potential data: A tutorial review. In D. Otto (Ed.), *Multidisciplinary perspectives in event-related brain potentials research* (pp. 555-572). Washington, DC: U.S. Environmental Protection Agency.

Gomes, H., Dunn, M., Ritter, W., Kurtzberg, D., Brattson, A., Kreuzer, J. A., Vaughan, H. G. Jr. (2001). Spatiotemporal maturation of the central and lateral N1 components to tones. *Developmental Brain Research,* 129, 147-155.

Gomot, M., Giard, M-H., Roux, S., Barthélémy, C., Bruneau, N. (2000). Maturation of frontal and temporal components of mismatch negativity (MMN) in children. *NeuroReport*, 11, 3109-3112.

Hyvärinen, A., & Oja, E. (2000). Independent component analysis: Algorithms and applications. Neural Networks, 13, 411-430.

Hämäläinen, J. A., Leppänen, P. H. T., Guttorm, T. K., Lyytinen, H. (2007). N1 and P2 components of auditory event-related potentials in children with and without reading disabilities. *Clinical Neurophysiology*, 118, 2263-2275.

Johnstone, S. J., Barry, R. J., Anderson, J. W., Coyle, S. F. (1996). Age-related changes in child and adolescence event-related component morphology, amplitude and latency to standard and target stimuli in an auditory oddball task. *International Journal of Psychophysiology*, 24, 223-238.

Karhu, J., Herrgård, E., Pääkkönen, A., Luoma, L., Airaksinen, E., Partanen, J. (1997). Dual cerebral processing of elementary auditory input in children. *NeuroReport*, 8, 1327-1330.

Kayser, J., Tenke, C. E., Bruder, G. E. (1998). Dissociation of ERP topographies for tonal and phonetic oddball tasks. *Psychophysiology*, 35, 576-590.

Kayser, J., & Tenke, C. E. (2003). Optimizing PCA methodology for ERP component identification and measurement: theoretical rationale and empirical evaluation. *Clinical Neurophysiology*, 114, 2307-2325.

Kayser, J., Tenke, C. E. (2005). Trusting in or braking with convention: Towards a renaissance of principal components analysis in electrophysiology. *Clinical Neurophysiology*, 116, 1747-1753.

Kayser, J., Tenke, C. E., Gates, N. A., Kroppmann, C. J., Gil, R. B., Bruder, G. E. (2006). ERP/CSD indices of impaired verbal working memory subprocesses in schizophrenia. *Psychophysiology*, 43, 237-252.

Kayser, J., & Tenke, C. E. (2006a). Principal component analysis of Laplacian waveforms as a generic method for identifying ERP generator patterns: I. Evaluation with auditory oddball tasks. *Clinical Neurophysiology*, 117, 348-368.

Kayser, J., & Tenke, C. E. (2006b). Principal component analysis of Laplacian waveforms as a generic method for identifying ERP generator patterns: II. Adequacy of low-density estimates. *Clinical Neurophysiology*, 117, 369-380.

Kurtzberg, D.,Vaughan, H. F., Kreuzer, J. A., Fliegler, K. Z. (1995). Developmental studies and clinical applications of mismatch negativity: Problems and prospects. *Ear Hear*, 105-117.

Law, S. K., Rohrbaugh, J. W., Adams, C. M., Eckardt, M. J. (1993). Improving spatial and temporal resolution in evoked EEG responses using surface Laplacians. *Electroencephalography and Clinical Neurophysiology*, 88, 309-322.

Leinonen, S., Müller, K., Leppänen, P. H. T., Aro, M., Ahonen, T., Lyytinen, H. (2001). Heterogeneity in adult dyslexic readers: relating processing skills to the speed and accuracy of oral text reading. *Reading and Writing*, 14, 265-296.

Makeig, S., Debener, S., Onton, J., Delorme, A. (2004). Mining event-related brain dynamics. *Trends in Cognitive Sciences*, 8, 204-210.

Nunez, P. (1981). Electric fields of the brain. New York: Oxford University Press.

Näätänen, R., & Picton, T. (1987). The N1 wave of the human electric and magnetic response to sound: a review and an analysis of the component structure. *Psychophysiology*, 24, 375-425.

Näätänen, R. (1989). Herätepotentiaalit ja kognitiiviset prosessit. *Psykologia*, 24, 436-449.

Näätänen, R. (1992). Event-related potentials and automatic information processing. *Attention and brain function*. Hillsdale, NJ: Lawrence Erlbaum.

Picton, T. W., Bentin, S., Berg, P., Donchin, E., Hillyard, S. A., Johnson, R., Jr., Miller, G. A., Ritter, W., Ruchkin, D. S., Rugg, M. D., Taylor, M. J. (2000). Guidelines for using human event-related potentials to study cognition: Recording standards and publication criteria. *Psychophysiology*, 37, 127-152.

Picton, T. W., Alain, C., Otten, L., Ritter, W., Achim, A. (2000). Mismatch negativity: Different water in the same river. *Audiology & Neuro-Otology*, 5, 111-139.

Ponton, C. W., Eggermont, J. J., Kwong, B., Don, M. (2000). Maturation of human central auditory system activity: evidence from multi-channel evoked potentials. *Clinical Neurophysiology*, 111, 220-236.

Ponton, C. W., Eggermont, J. J., Khosla, D., Kwong, B., Don, M. (2002). Maturation of human central auditory system activity: separating evoked potentials by dipole source modeling, *Clinical Neurophysiology*, 113, 407-420.

Richards, J. E. (2004). Recovering dipole sources from scalp-recorded event-related potentials using component analysis: principal component analysis and independent component analysis. *International Journal of Psychophysiology*, 54, 201-220.

Spencer, K. M., Dien, J., Donchin, E. (1999). A Componential analysis of the ERP elicited by novel events using dense electrode array. *Psychophysiology*, 36, 409-414.

Spencer, K. M., Dien, J., Donchin, E. (2001). Spatiotemporal analysis of the late ERP responses to deviant stimuli. *Psychophysiology*, 38, 343-358.

Tenke, C. E., Kayser, J., Fong, R., Leite, P., Towey, J. P., Bruder, G. E. (1998). Response- and stimulus-related ERP asymmetries in a tonal oddball task: A Laplacian analysis. *Brain Topography*, 10, 201-210.

Tenke, C. E., & Kayser, J. (2005). Reference-free quantification of EEG spectra: Combining current source density (CSD) and frequency principal component analysis (fPCA). *Clinical Neurophysiology*, 116, 2826-2846.

Tonnquist-Uhlen, I., Ponton, C. W., Eggermont, J. J., Kwong, B., Don, M. (2003). Maturation of human central auditory system activity: T-complex. *Clinical Neurophysiology*, 114, 685-701.

Tucker, D. M. (1993). Spatial sampling of head electrical fields: The geodesic sensor net. *Electroencephalography and Clinical Neurophysiology*, 87, 154-163.

Wallstrom, G. L., Kass, R. E., Miller, A., Cohn, J. F., Fox, N. A. (2004). Automatic correction of ocular artefacts in the EEG: a comparison of regression-based and component-based methods. *International Journal of Psychophysiology*, 53, 105-119.

Wood, C. C., & McCarthy, G. (1984). Principal component analysis of event-related potentials: simulation studies demonstrate misallocation of variance across components. *Electroencephalography and Clinical Neurophysiology*, 59, 249-260.